Cyclic organohydroborate complexes of metallocenes
VIII. Triphenylsiloxy derivatives of Group IV organometallic systems, $Cp_2M(OSiPh_3)X$ (M = Ti, Zr, Hf; X = Cl, $\{(\mu\text{-}H)_2BC_8H_{14}\}$)

Fabrice Lacroix, Christine E. Plecnik, Shengming Liu, Fu-Chen Liu,
Edward A. Meyers, Sheldon G. Shore *

Department of Chemistry, Newman and Wolfrom Laboratory, The Ohio State University, 100 West 18th Avenue, Columbus, OH 43210-1185, USA

Abstract

Group IV metallocene triphenylsiloxy chlorides, $Cp_2MCl(OSiPh_3)$ (**1**, M = Ti; **2**, M = Zr; **3**, M = Hf), and cyclic organohydroborates, $Cp_2M(OSiPh_3)\{(\mu\text{-}H)_2BC_8H_{14}\}$ (**4**, M = Zr; **5**, M = Hf), were synthesized and characterized. The new hafnocene chloride derivative **3** was obtained by treating Cp_2HfCl_2 with triphenylsilanol and piperidine. The 18-electron cyclic organohydroborates **4** and **5** were afforded by reacting **2** and **3** with $K[H_2BC_8H_{14}]$, the potassium salt of the 9-BBN dimer. Reaction of **1** with $K[H_2BC_8H_{14}]$ causes reduction of the Ti(IV) center and produces the well-known Ti(III), 17-electron, paramagnetic dimer $[Cp_2Ti(\mu\text{-}Cl)_2TiCp_2]$ (**6**). Single-crystal X-ray diffraction structures of **3**, **4**, **5**, and **6** were determined.
© 2003 Elsevier B.V. All rights reserved.

Keywords: Group IV metallocene; Triphenylsiloxy; Organohydroborate; Silica model

1. Introduction

Grafting [1,2] organometallic systems onto a support's surface has been one advancement in the field of surface organometallic chemistry [3]. Recently, Basset and co-workers designed ethylene polymerization catalysts by grafting zirconocene alkyl fragments onto the surface of silica [1a]. Supported catalysts such as these can be a challenge to study in terms of understanding reactivity/activity and deciphering structure [3]. More simplified and easily characterized homogeneous analogues that attempt to simulate the silanol surface of partially dehydroxylated silica have been developed. Reasonable models of isolated silanol sites (≡Si–OH) can be based on silsesquioxane [4,5] and triphenylsiloxy ligands [5b].

In addition to their ability to selectively reduce organic functionalities (i.e. aldehydes and ketones) [6], organohydroborate anions are capable of ligating to metals in a manner similar to that of tetrahydroborate [7]. For instance, this laboratory has employed cyclic organohydroborate anions $[H_2BR_2]^-$ ($R_2 = C_4H_8$, C_5H_{10}, C_8H_{14}) as bidentate ligands (two M–H–B bridges) to a variety of metallocenes (M = Ti, Zr, Hf, Nb) [8]. The properties and reactivity of organohydroborate complexes differentiate them from the tetrahydroborate analogues. (1) The intramolecular hydrogen exchange of bridging and Cp hydrogens can be readily investigated without the interference of a B–H_b and B–H_t fluxional process [8d,8h,9]. (2) The chemistry of the bridging hydrogens is more easily explored without the complication of terminal hydrogen (B–H_t) reactions. The reactivity of metallocene organohydroborates with $B(C_6F_5)_3$ is of particular interest because this Lewis acid is a typical co-catalyst in metal-catalyzed olefin polymerization and is a traditional alkyl carbanion abstract-

---

ing reagent [10]. Previous work demonstrates that the bridging hydrogens in metallocene cyclic organohydroborates are abstracted by $B(C_6F_5)_3$ [11], and resulting products include metallocene cations, which have the potential to function as olefin polymerization catalysts [12]. The present contribution describes the preparation of new models of potential homogeneous single-site metallocene anchored catalysts, namely, triphenylsilanolato derivatives of Group IV metallocene cyclic organohydroborates, $Cp_2M(OSiPh_3)\{(\mu\text{-}H)_2BC_8H_{14}\}$.

2. Results and discussion

2.1. Preparation of $Cp_2MCl(OSiPh_3)$ $(M = Ti, Zr, Hf)$

Group IV metallocene chloro triphenylsilanolates $Cp_2MCl(OSiPh_3)$ (**1**, M = Ti; **2**, M = Zr; **3**, M = Hf) were synthesized by reacting the corresponding metallocene dichloride with triphenylsilanol and piperidine (Eq. (1)) [13].
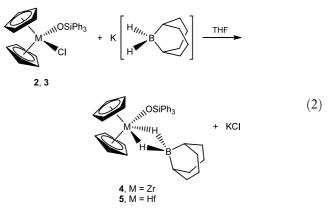

$$(1)$$

1, M = Ti
2, M = Zr
3, M = Hf

Compounds **1** and **2** were first prepared according to this procedure by Dehnicke and co-workers [13]. The synthetic method was extended to Cp_2HfCl_2, and a new hafnocene compound **3** was isolated in 56% yield. The molecular structure of **3** was determined by single-crystal X-ray diffraction analysis. Compounds **1**, **2**, and **3** were characterized by ^{1}H- and ^{13}C-NMR spectroscopies. Cyclopentadienyl protons appear at around δ 5.9 and two multiplets centered at δ 7.8 and 7.2 are observed for the phenyl ring hydrogens. The ^{13}C-NMR spectra possess four resonances for the phenyl carbons and one for the Cp nuclei. The IR spectrum of **3** possesses a Hf–O–Si stretch at 977 cm^{-1} [14], which is close to the 957 cm^{-1} frequency recorded for both **1** and **2** [13].

2.2. Reactions of 1, 2, and 3 with $K[H_2BC_8H_{14}]$

2.2.1. Preparation of $Cp_2M(OSiPh_3)\{(\mu\text{-}H)_2BC_8H_{14}\}$ $(M = Zr, Hf)$

Metathesis reactions of **2** and **3** with $K[H_2BC_8H_{14}]$ (the hydroborate anion of the 9-BBN dimer, $(\mu\text{-}H)_2(BC_8H_{14})_2$) [15] afforded the metallocene triphenyl-

siloxy cyclic organohydroborates $Cp_2M(OSiPh_3)\{(\mu\text{-}H)_2BC_8H_{14}\}$ (**4**, M = Zr; **5**, M = Hf; Eq. (2)).
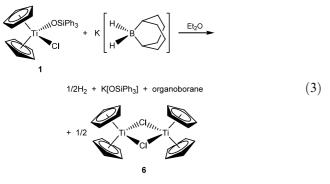

$$(2)$$

4, M = Zr
5, M = Hf

The anion $[H_2BC_8H_{14}]^-$ displaces Cl$^-$ and binds to Zr and Hf in a bidentate fashion through three-center, two-electron M–H–B bonds. The driving force of this reaction is KCl precipitation. The reaction is complete within minutes and no side products are observed by ^{11}B-NMR spectroscopy. Attempts to synthesize pure sample of another triphenylsilanolato derivative of a zirconocene cyclic organohydroborate, $Cp_2Zr(OSiPh_3)\{(\mu\text{-}H)_2BC_5H_{10}\}$, were unsuccessful [16]. The complex $Cp_2ZrH\{(\mu\text{-}H)_2BC_5H_{10}\}$ was combined with Ph_3SiOH and the resulting mixture of products, including the desired compound and $Cp_2Zr(OSiPh_3)_2$, could not be separated [16]. It appears that the most facile route toward the zirconocene and hafnocene triphenylsiloxy organohydroborates is through $Cp_2MCl(OSiPh_3)$.

Compounds **4** and **5** are 18-electron, diamagnetic species. In C_6D_6, the ^{11}B-NMR resonances of the organohydroborate ligand appear as unresolved broad peaks at 5.6 ppm for **4** and 2.3 ppm for **5**. The signals for **4** and **5** are upfield comparing with those of the ^{11}B-NMR resonances of $Cp_2ZrCl\{(\mu\text{-}H)_2BC_8H_{14}\}$ (17.7 ppm) [8h], $Cp_2ZrH\{(\mu\text{-}H)_2BC_8H_{14}\}$ (32.5 ppm) [8h], $Cp_2HfCl\{(\mu\text{-}H)_2BC_4H_8\}$ (12.4 ppm) [8a,8b], and $Cp_2HfCl\{(\mu\text{-}H)_2BC_5H_{10}\}$ (9.3 ppm) [8c]. The two bridging protons are inequivalent. One bridging hydrogen peak is broad and upfield at -0.3 ppm for **4** and $+0.5$ ppm for **5**. The other bridging hydrogen is obscured by the multiplet (δ 2.3 to 1.7) for the β- and γ-protons of the organohydroborate ring. The chemical shift of α-protons is ca. 1.5 ppm, and the peaks are broad due to the quadrupolar ^{11}B nuclei [8g]. The proton assignments are based on integration and a carbon-detected ^{1}H-^{13}C-NMR correlation experiment (HETCOR). Phenyl and Cp proton signals for **4** and **5** are slightly shifted relative to those of **1** and **2**.

2.2.2. Formation of $[Cp_2Ti(\mu\text{-}Cl)_2TiCp_2]$ (6)

Complex **1** and $K[H_2BC_8H_{14}]$ were mixed in a 1:1 molar ratio in Et_2O (Eq. (3)). The reaction solution progressively changed color from orange to purple then

to dark green with evolution of hydrogen, all of which are indications of Ti(IV) reduction to Ti(III). The reaction was monitored by ^{11}B-NMR, and after 15 min the spectrum contained two peaks at 60.8 and 28.8 ppm. After several hours the latter signal, assigned to the 9-BBN dimer [8g,8h], disappeared and the peak at 60.8 ppm remained. This downfield chemical shift is characteristic of a trialkyl borane [17]. Green crystals were isolated from the reaction solution, and single-crystal X-ray diffraction analysis revealed that the titanocene product is the paramagnetic, Ti(III), chlorine-bridged dimer $[Cp_2Ti(\mu\text{-}Cl)_2TiCp_2]$ (6) [18]. Proton- and ^{13}C-NMR spectra of 6 are not valid due to the paramagnetism of the Ti(III) centers 7e[8g,11b].

The production of 6 most likely occurs in a stepwise fashion:

1) Metathesis. Displacement of $[OSiPh_3]^-$ with $[H_2BC_8H_{14}]^-$ causes precipitation of $K[OSiPh_3]$ and perhaps forms the intermediate $[Cp_2TiCl\{(\mu\text{-}H)_2BC_8H_{14}\}]$. This metathetical step contrasts the substitution of Cl^- by $[H_2BC_8H_{14}]^-$ in the zirconocene and hafnocene triphenylsilanolates (Eq. (2)). It is not immediately clear why replacement of $[OSiPh_3]^-$ is favored over Cl^- in the titanocene system. However, a comparison of the average M–OR and M–Cl bonds dissociation enthalpies may shed light on the result; Ti–OR and Ti–Cl bonds have similar dissociation energies, whereas Zr–OR and Hf–OR bonds are on average stronger than the corresponding Zr–Cl and Hf–Cl bonds [19].

2) Redox. Although the identity of the actual reducing agent is unknown, reduction of Ti(IV) to Ti(III) is not surprising. For example, tetrahydroborate [20] and organohydroborates [8g] readily reduce Cp_2TiCl_2 to yield Ti(III) complexes $Cp_2Ti\{(\mu\text{-}H)_2BR_2\}$ ($R_2 = H_2$, C_4H_8, C_5H_{10}, C_8H_{14}). The unidentified trialkyl borane product in Eq. (3) probably results from rearrangement of the alkyl groups in the 9-BBN dimer [21]. Chlorine bridges are constructed to relieve electron deficiency at the two Ti(III) centers.

2.3. Molecular structures

The molecular structures of 3–6 were determined by single-crystal X-ray diffraction analysis; structures are shown in Figs. 1–4. Crystallographic data and selected bond distances and angles are compiled in Tables 1–4. The structures of 1 and 2 were reported by Dehnicke and co-workers [13]. Complexes 2 and 3 crystallize in the same trigonal space group, $P\bar{3}$. The structure of 6 was originally elucidated by Stucky and co-workers [18]. However, when crystals are grown under different conditions, 6 exists in a different crystalline form (i.e. a polymorph with different crystal symmetry and unit cell parameters). Nevertheless, bond distances and angles (Table 4) for the two polymorphs are nearly identical, and the structures will not be discussed further (see Section 3). Crystals of 6 are twinned.

The coordination geometry about the Zr and Hf atoms in 3, 4, and 5 is best described as a distorted tetrahedron, with the two Cp centroids, the oxygen atom of $[OSiPh_3]^-$, and Cl or B located at the corners of the tetrahedron. Structural features in 1–3 are comparable (Table 2), and this is reflected by the narrow M–O (1.842(4)–1.961(6) Å) and M–Cl (2.388(2)–2.460(3) Å) ranges [13]. In compounds 4 and 5, the $Cp_2M(OSiPh_3)$ fragment bonds to the $\{BC_8H_{14}\}$ moiety through two bridging hydrogens. Metal···boron distances (Table 3) in 4 (2.71(1) Å) and 5 (2.624(8) Å) are slightly elongated relative to those in other zirconocene and hafnocene organohydroborates, $Cp_2ZrCl\{(\mu\text{-}H)_2BC_8H_{14}\}$ (2.593(3), 2.609(3) Å) [8h], $Cp_2ZrH\{(\mu\text{-}H)_2BC_8H_{14}\}$ (2.566(2) Å) [8h], and $Cp_2HfCl\{(\mu\text{-}H)_2BC_4H_8\}$ (2.527(5) Å) [8b]. This may be a consequence of the larger steric bulk of the $[OSiPh_3]^-$ ligand compared to Cl^- and H^-. The $M–H_b$ and $B–H_b$ bond lengths are typical for metallocene organohydroborates [8b,8h]. In compounds 1–5 the short M–O distances (3, 1.934(5) Å; 4, 1.985(3) Å; 5, 1.993(4) Å) and nearly linear M–O–Si angles (3, 171.9(4)°; 4, 159.4(2)°; 5, 158.3(3)°) suggest
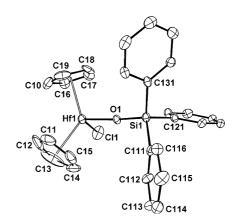

Fig. 1. Molecular structure of one of the three independent molecules of $Cp_2HfCl(OSiPh_3)$ (3) showing 25% probability thermal ellipsoids. Hydrogen atoms are omitted for clarity.
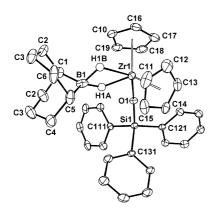
Fig. 2. Molecular structure of Cp$_2$Zr(OSiPh$_3$){(μ-H)$_2$BC$_8$H$_{14}$} (**4**) showing 10% probability thermal ellipsoids. Hydrogens attached to carbon atoms are omitted for clarity.
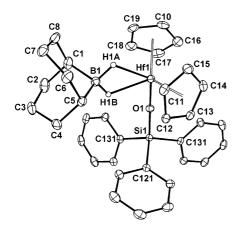

Fig. 3. Molecular structure of Cp$_2$Hf(OSiPh$_3$){(μ-H)$_2$BC$_8$H$_{14}$} (**5**) showing 25% probability thermal ellipsoids. Hydrogens attached to carbon atoms are omitted for clarity.
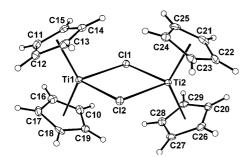

Fig. 4. Molecular structure of one of the two independent molecules of [Cp$_2$Ti(μ-Cl)$_2$TiCp$_2$] (**6**) showing 25% probability thermal ellipsoids. Hydrogen atoms are shown with arbitrary thermal ellipsoids.

p$_\pi$–d$_\pi$ bonding (electron donation from occupied oxygen p orbitals of [OSiPh$_3$]$^-$ into empty metal d orbitals) [13,22]. The extent of this p$_\pi$–d$_\pi$ bonding appears to be stronger in **1**, **2**, and **3**; the electron withdrawing effect of Cl$^-$, in contrast to the electron donating ability of [H$_2$BC$_8$H$_{14}$]$^-$, encourages greater donation from [OSiPh$_3$]$^-$ to the metal. Similar p$_\pi$–d$_\pi$ interactions are

observed in the bis(triphenylsiloxy)-substituted systems (DME)ZrCl$_2$(OSiPh$_3$)$_2$ (Zr–O, 1.91(1) Å; Zr–O–Si, 171(1)°) [22] and Cp″ZrCl(OSiPh$_3$)$_2$ (Cp″ = 1,3-C$_5$H$_3$(SiMe$_3$)$_2$; Zr–O, 1.921(4), 1.929(5) Å; Zr–O–Si, 175.3(3), 159.3(2)°) [5b].

3. Experimental

3.1. General procedures

All manipulations were carried out on a standard high vacuum line or in a dry box under an atmosphere of nitrogen. Diethyl ether, tetrahydrofuran, and toluene were dried over sodium-benzophenone and freshly distilled prior to use. Hexane was stirred over concentrated sulfuric acid for 2 days and then decanted and washed with water. Next, the hexane was stirred over sodium-benzophenone for 1 week, followed by distillation into a storage bulb-containing sodium-benzophenone. Cp$_2$TiCl$_2$, Cp$_2$ZrCl$_2$, Cp$_2$HfCl$_2$, and Ph$_3$SiOH were purchased from Aldrich and used as received. Piperidine was purchased from Aldrich, dried over sodium-benzophenone, and freshly distilled prior to use. K[H$_2$BC$_8$H$_{14}$] was prepared by the literature procedure [15]. The synthesis of Cp$_2$MCl(OSiPh$_3$) (**1**, **2**), originally prepared by Dehnicke and co-workers [13], was slightly modified and is detailed below. Elemental analyses were obtained by Galbraith Laboratories, Knoxville, TN. ^{1}H-NMR spectra were obtained on Bruker AM-250 and DPX-400 spectrometers operating at 250.1 and 400.1 MHz, respectively, and referenced to residual solvent protons. ^{13}C-NMR spectra were obtained on Bruker AM-250 and DPX-400 spectrometers operating at 63.0 or 100.6 MHz, respectively, and referenced to deuterated solvent signals. ^{11}B-NMR spectra were obtained on a Bruker AM-250 spectrometer operating at 80.3 MHz and externally referenced to BF$_3$·OEt$_2$ in C$_6$D$_6$ ($\delta = 0.00$ ppm). Infrared spectra were recorded on a Mattson Polaris Fourier Transform Spectrometer with 2 cm^{-1} resolution.

3.2. X-ray structure determination

Single-crystal X-ray diffraction data were collected on a Nonius Kappa CCD diffraction system, which employs graphite-monochromated Mo–K$_\alpha$ radiation ($\lambda = 0.71073$ Å). A single crystal of **3**, **4**, **5**, and **6** was mounted on the tip of a glass fiber coated with Fomblin oil (a pentafluoropolyether). Unit cell parameters were obtained by indexing the peaks in the first 10 frames and refined employing the whole data set. All frames were integrated and corrected for Lorentz and polarization effects using the DENZO-SMN package (Nonius BV, 1999) [23]. Absorption correction was applied using the SORTAV program [24] provided by MaXus software [25].

Table 1

Crystal and structure refinement data for $Cp_2HfCl(OSiPh_3)$ (3), $Cp_2Zr(OSiPh_3)\{(\mu-H)_2BC_8H_{14}\}$ (4), $Cp_2Hf(OSiPh_3)\{(\mu-H)_2BC_8H_{14}\}$ (5), and $[Cp_2Ti(\mu-Cl)_2TiCp_2]$ (6)

	$3\cdot1/6C_5H_{11}N$	4	5	6
Empirical formula	$C_{28.833}H_{26.833}N_{0.167}ClHfOSi$	$C_{36}H_{41}BOSiZr$	$C_{76}H_{90}B_2Hf_2O_3Si_2$	$C_{20}H_{20}Cl_2Ti_2$
Formula weight (amu)	633.73	619.81	1486.26	427.06
Temperature (°C)	−73	−10	−73	−73
Crystal system	Trigonal	Triclinic	Monoclinic	Triclinic
Space group	$P\bar{3}$	$P1$	$P2_1/c$	$P\bar{1}$
Crystal color, habit	Colorless rectangle	Colorless block	Colorless rectangle	Dark green block
a (Å)	35.457(1)	9.116(1)	8.688(1)	11.393(1)
b (Å)	35.457(1)	9.695(1)	17.916(1)	11.396(1)
c (Å)	10.443(1)	10.696(1)	21.138(1)	13.541(1)
α (°)	90	116.11(1)	90	89.98(1)
β (°)	90	92.12(1)	90.00(1)	89.91(1)
γ (°)	120	105.92(1)	90	89.63 (1)
V (Å³)	11371(1)	802.6(1)	3290.2(4)	1758.0(3)
Z	18 [a]	1	4	4 [b]
D_{calc} (g cm⁻³)	1.671	1.282	1.427	1.614
μ (mm⁻¹)	4.302	0.406	3.232	1.210
Crystal size (mm)	$0.23 \times 0.15 \times 0.06$	$0.15 \times 0.08 \times 0.08$	$0.27 \times 0.19 \times 0.12$	$0.19 \times 0.19 \times 0.15$
2θ Range (°)	2.30–50.04	4.72–49.84	4.54–50.06	5.86–50.06
Index ranges	$-42 \leq h \leq 41, -42 \leq k \leq 41, -12 \leq l \leq 12$	$-10 \leq h \leq 10, -11 \leq k \leq 11, -12 \leq l \leq 12$	$-10 \leq h \leq 10, -21 \leq k \leq 21, -25 \leq l \leq 25$	$-13 \leq h \leq 13, -13 \leq k \leq 13, -16 \leq l \leq 15$
Reflections collected	66 407	17 422	69 718	9996
Independent reflections	13 374	5443	5823	5807
R_{int}	0.1174	0.1288	0.0482	0.0187
Completeness to θ (%)	99.8	99.7	99.9	93.6
Max/min transmission	0.7824, 0.4378	0.9682, 0.9416	0.6977, 0.4757	0.8393, 0.8027
Data/restraints/parameters	13 374/0/902	5443/3/369	5823/0/369	5807/0/429
$R_1 [I \geq 2.0\sigma(I)]$ [c]	0.0587	0.0486	0.0229	0.0265
wR_2 (all data) [d]	0.1082	0.1367	0.0604	0.0639
Goodness-of-fit on F^2	1.185	1.393	1.076	1.040
Largest difference peak and hole (e Å⁻³)	1.371, −0.801	0.490, −0.683	1.014, −1.194	0.292, −0.348

[a] In the asymmetric unit cell, there are three independent molecules of 3, 1/3 of a molecule of $C_5H_{11}N$, and 1/6 of another molecule of $C_5H_{11}N$.

[b] There are two independent molecules in the asymmetric unit cell.

[c] $R_1 = \Sigma||F_o| - |F_c||/\Sigma|F_o|$.

[d] $wR_2 = \{\Sigma w(F_o^2 - F_c^2)^2/\Sigma w(F_o^2)^2\}^{1/2}$.

Table 2

Selected bond distances (Å) and angles (°) for $Cp_2MCl(OSiPh_3)$ (1, M = Ti; 2, M = Zr; 3, M = Hf)

	1 [a]	2 [a,b]	3 [b]
Bond distances			
Average M−C	2.381[10] [c]	2.510[8]	2.482[8]
M−Centroid	2.076(1), 2.072(1)	2.213(7), 2.220(6)	2.208, 2.202
M−O	1.842(4)	1.961(6)	1.934(5)
M−Cl	2.388(2)	2.460(3)	2.441(3)
Bond angles			
Centroid−M−Centroid	132.6(1)	127.7(3)	127.9
M−O−Si	164.5(2)	173.0(4)	171.9(4)
O−M−Cl	95.9(1)	98.4(2)	97.3(2)

[a] Ref. [13].

[b] There are three independent molecules in the asymmetric unit cell. Data are listed for only one molecule.

[c] Ref. [28].

Structures were solved by direct methods and refined using SHELXTL-97 (difference electron density calculation, full-matrix least-squares refinements) structure solution package [26]. Data merging was performed using the data preparation program supplied by SHELXTL-97. For each structure, non-hydrogen atoms were located and refined anisotropically. Bridging hydrogen atoms in 4 and 5 were located and refined isotropically. All other hydrogen atom positions were calculated using standard geometries.

Piperidine co-crystallizes with 3 (before crystallization, the solid was not washed with hexane). In the asymmetric unit cell, there are three unique molecules of 3, 1/3 of a molecule of $C_5H_{11}N$ (N(1), N(2); threefold rotation about an axis passing through the center of the piperidine ring generates the entire molecule), and 1/6 of another molecule of $C_5H_{11}N$ (N(3); inversion and threefold rotation about the center of the ring generates the entire molecule). In the unit cell, there are 18

Table 3
Selected bond distances (Å) and angles (°) for $Cp_2M(OSiPh_3)\{(\mu\text{-}H)_2BC_8H_{14}\}$ (**4**, M = Zr; **5**, M = Hf)

	4	5
Bond distances		
Average M(1)–C(11–15)	2.535[8]	2.516[4]
Average M(1)–C(16–10)	2.521[9]	2.514[7]
M(1)–Centroid$_{(C11-C15)}$	2.251	2.214
M(1)–Centroid$_{(C16-C10)}$	2.225	2.214
M(1)–O(1)	1.985(3)	1.993(4)
M(1)···B(1)	2.71(1)	2.624(8)
M(1)–H(1A)	1.74(3)	2.14(8)
M(1)–H(1B)	2.12(7)	2.06(7)
B(1)–H(1A)	1.10(4)	1.10(7)
B(1)–H(1B)	1.22(8)	1.07(8)
O(1)–Si(1)	1.614(3)	1.608(4)
Bond angles		
M(1)–O(1)–Si(1)	159.4(2)	158.3(3)
O(1)–M(1)–B(1)	102.2(2)	102.9(2)
O(1)–M(1)–H(1A)	89(1)	127(2)
O(1)–M(1)–H(1B)	128(2)	80(2)
H(1A)–M(1)–H(1B)	39(2)	46(3)
H(1A)–B(1)–H(1B)	71(4)	100(6)
Centroid–M(1)–Centroid	126.4	129.8

Table 4
Selected bond distances (Å) and angles (°) for $[Cp_2Ti(\mu\text{-}Cl)_2TiCp_2]$ (**6**)

Bond distances			
Ti(1)···Ti(2)	3.912	Ti(3)···Ti(4)	3.908
Cl(1)···Cl(2)	3.283	Cl(3)···Cl(4)	3.276
Ti(1)–Cl(1)	2.551(1)	Ti(1)–Cl(2)	2.546(1)
Ti(2)–Cl(1)	2.558(1)	Ti(2)–Cl(2)	2.560(1)
Average Ti–Cl	2.552[3]	Average Ti–C	2.385[2]
Ti(1)–Centroid$_{(C11-C15)}$	2.067	Ti(1)–Centroid$_{(C16-C10)}$	2.068
Ti(2)–Centroid$_{(C21-C25)}$	2.060	Ti(2)–Centroid$_{(C26-C20)}$	2.063
Bond angles			
Cl(1)–Ti(1)–Cl(2)	80.22(3)	Cl(1)–Ti(2)–Cl(2)	79.81(3)
Ti(1)–Cl(1)–Ti(2)	99.95(3)	Ti(1)–Cl(2)–Ti(2)	100.02(3)
Centroid–Ti(1)–Centroid	132.2	Centroid–Ti(2)–Centroid	131.3
Centroid$_{(C11-C15)}$–Ti(1)–Cl(1)	107.4	Centroid$_{(C11-C15)}$–Ti(1)–Cl(2)	108.3
Centroid$_{(C16-C10)}$–Ti(1)–Cl(1)	108.9	Centroid$_{(C16-C10)}$–Ti(1)–Cl(2)	107.7

molecules of **3** and three molecule of $C_5H_{11}N$. The piperidine molecules are disordered because of symmetry. As a result, all atoms and their occupancies were refined as nitrogens (N(1), 92% site occupancy factor; N(2), 88% site occupancy factor; N(3), 85% site occupancy factor). These site occupancy factors are close to the theoretical value of 88%. Due to the disorder, hydrogen atom positions were not calculated. Two independent molecules of **3** have disordered Hf atoms; that is, the atoms adopt two alternate positions (Hf(2), Hf(2′); Hf(3), Hf(3′)). Atoms Hf(1), Hf(2), and Hf(3) were refined anisotropically and have 100, 91, and 97%

site occupancy factors, respectively. The disordered sites, Hf(2′) and Hf(3′), were refined isotropically and possess 9 and 3% site occupancy factors, respectively.

Disordered THF solvent co-crystallizes with **5**. In the asymmetric unit, there is one molecule of **5** and one half of a THF molecule (two carbons, C_a, C_b, and an oxygen (50% s.o.f.). The full THF molecule is represented by two molecules, each of half occupancy, which share their four carbon atoms C_a, C_b, $C_{a'}$, and $C_{b'}$ that are generated through an inversion center that is located in the center of the four carbons.

The molecular structure of **6** was previously determined by Stucky and co-workers [18]. Crystals were grown by sublimation and data were collected at room temperature (r.t.). The structure was solved in the monoclinic space group $P2_1/c$ ($a = 13.422(8)$, $b = 15.666(11)$, $c = 13.083(12)$ Å, $\beta = 94.21(4)°$), and there are 1.5 independent molecules of **6** in the asymmetric unit. The authors noted that crystals grown from benzene solutions were twinned and exhibited pseudo-fourfold symmetry. The space group of these could not be determined, and the unit cell was not reported.

In the present work, crystals of **6** were isolated from an Et_2O solution and data were collected at -73 °C. The resulting unit cell has triclinic symmetry $P\bar{1}$ ($a = 11.393(1)$, $b = 11.396(1)$, $c = 13.541(1)$ Å, $\alpha = 89.98(1)$, $\beta = 89.91(1)$, $\gamma = 89.63(1)°$), with two unique molecules in the asymmetric unit. Therefore, **6** can exist in two different crystalline forms (i.e. polymorphs). Although the unit cell parameters indicate tetragonal symmetry (a and b are nearly equal and α, β, and γ are almost 90°), there are no reflection conditions. The appearance of pseudo-fourfold symmetry is a result of twinning. The two parts of the twinned crystal are related by rotation; a 180° rotation of the parent unit cell through the $[-1, 1, 0]$ axis generates the twin. The twin law was determined by the ROTAX program [27]. The fractional contribution of the twin component was refined and found to be 33.2%.

3.3. Preparation of $Cp_2TiCl(OSiPh_3)$ (**1**)

A 150 ml flask was charged with 1.369 g (5.50 mmol) of Cp_2TiCl_2 and 70 ml of Et_2O. About 5 ml of THF was added to mostly dissolve the Cp_2TiCl_2. A solution of Ph_3SiOH (1.380 g, 5.00 mmol) in 10 ml of Et_2O was slowly added dropwise to the Cp_2TiCl_2 solution with stirring. Piperidine (0.56 ml, 5.5 mmol) was added using a plastic syringe. The reaction mixture was stirred for 6 h. After filtration, the volatiles were removed under dynamic vacuum, and an orange-red powder was obtained. The powder was dissolved in 30 ml of toluene. Slow evaporation of the toluene at r.t. (until 5 ml of solution remained) yielded orange crystals. The mother liquor was removed and the crystals were washed with 2×5 ml of hexane. After vacuum drying for 12 h, 1.340

g (55% yield) of **1** was isolated. ^{1}H-NMR (250 MHz, C_6D_6): δ 7.86-7.82 (m, 6H, Ph), 7.26-7.23 (m, 9H, Ph), 5.92 (s, 10H, Cp). ^{13}C-NMR (63 MHz, C_6D_6): δ 137.9 (s, Ph), 136.0 (s, Ph), 130.0 (s, Ph), 128.3 (s, Ph), 118.0 (s, Cp).

3.4. Preparation of Cp₂ZrCl(OSiPh₃) (2)

In a procedure similar to the one described above for **1**, 1.608 g (5.50 mmol) of Cp_2ZrCl_2, 1.379 g (5.00 mmol) of Ph_3SiOH, and 0.57 ml (5.5 mmol) of piperidine afforded 2.112 g (79% yield) of **2** as colorless crystals. ^{1}H-NMR (250 MHz, C_6D_6): δ 7.82-7.78 (m, 6H, Ph), 7.25-7.23 (m, 9H, Ph), 5.90 (s, 10H, Cp). ^{13}C-NMR (63 MHz, C_6D_6): δ 137.4 (s, Ph), 135.6 (s, Ph), 129.9 (s, Ph), 128.2 (s, Ph), 114.4 (s, Cp).

3.5. Preparation of Cp₂HfCl(OSiPh₃) (3)

In a procedure similar to the one described above for **1**, 2.089 g (5.50 mmol) of Cp_2HfCl_2, 1.381 g (5.00 mmol) of Ph_3SiOH, and 0.56 ml (5.5 mmol) of piperidine afforded 1.740 g (56% yield) of **3** as colorless crystals. ^{1}H-NMR (250 MHz, C_6D_6): δ 7.82-7.78 (m, 6H, Ph), 7.25-7.22 (m, 9H, Ph), 5.84 (s, 10H, Cp). ^{13}C-NMR (63 MHz, C_6D_6): δ 137.5 (s, Ph), 135.6 (s, Ph), 129.9 (s, Ph), 128.2 (s, Ph), 113.2 (s, Cp). IR (KBr, cm^{-1}): 3109 (w), 3065 (w), 3046 (w), 3019 (w), 1968 (vw), 1895 (vw), 1830 (vw), 1739 (vw), 1675 (vw), 1623 (vw), 1588 (m), 1567 (vw), 1483 (m), 1427 (s), 1388 (w, sh), 1367 (w), 1332 (vw), 1306 (w), 1261 (mw), 1185 (mw), 1160 (mw, sh), 1116 (s), 1066 (w), 1013(s, sh), 1001 (s, sh), 977 (s), 814 (s), 744 (s), 704 (s), 619 (w), 530 (ms, sh), 511 (s). Anal. Calc. for $C_{28}H_{25}ClHfOSi$: C, 54.28; H, 4.08. Found: C, 53.80; H, 4.15%.

3.6. Preparation of Cp₂Zr(OSiPh₃){(μ-H)₂(BC₈H₁₄)} (4)

In a 50 ml flask, a solution of $K[H_2BC_8H_{14}]$ (0.225 g, 1.39 mmol) in 10 ml of THF was added dropwise to a solution of **2** (0.737 g, 1.39 mmol) in 20 ml of THF. The reaction mixture was stirred for 1 h. The solvent was removed under dynamic vacuum, and 25 ml of THF was vacuum transferred into the flask. The solution was filtered to remove KCl, THF was evaporated, and a white foamy solid was obtained. The solid was dissolved in 20 ml of toluene and crystals were grown by slowly evaporating the solvent until 2 ml of solution remained. After removal of the mother liquor, the crystal were washed with 5 ml of hexane and vacuum dried for 12 h. Compound **4** (0.450 g, 52% yield) was isolated as white crystals. ^{11}B-NMR (80 MHz, C_6D_6): δ 5.6 (br t). ^{1}H-NMR (400 MHz, C_6D_6): δ 7.74-7.70 (m, 6H, Ph), 7.27-7.24 (m, 9H, Ph), 5.82 (s, 10H, Cp), 2.28-1.74 (m, 13H, β-, γ-, μ-H), 1.50 (br s, 2H, α-H), -0.3 (br s, 1H, μ-H).

^{13}C-NMR (101 MHz, d_8-THF): δ 138.7 (s, Ph), 136.0 (s, Ph), 130.0 (s, Ph), 128.4 (s, Ph), 112.6 (s, Cp), 34.4 (s, β-C), 28.3 (br s, α-C), 25.6 (br s, γ-C). IR (KBr, cm^{-1}): 3101 (vw), 3064 (w), 3046 (w), 3023 (vw), 2980 (w), 2913 (m, sh), 2867 (s), 2823 (ms, sh), 2665 (vw), 2052 (mw, sh), 2021 (m), 1943 (mw), 1899 (w), 1827 (vw), 1495 (mw), 1428 (m), 1370 (m), 1339 (m), 1291 (m), 1203 (mw), 1110 (ms), 1071 (mw), 1051 (m), 1023 (m), 1015 (m), 961 (vs), 811 (vs), 745 (m), 703 (s), 511 (ms). Anal. Calc. for $C_{36}H_{41}BOSiZr$: C, 69.76; H, 6.67; Si, 4.53. Found: C, 69.16; H, 6.92; Si, 4.44%.

3.7. Preparation of Cp₂Hf(OSiPh₃){(μ-H)₂(BC₈H₁₄)} (5)

In a procedure similar to the one described above for **4**, 0.622 g (1.00 mmol) of **3** and 0.162 g (1.00 mmol) of $K[H_2BC_8H_{14}]$ were reacted in THF. Colorless needlelike crystals of **5** (0.380 g, 54% yield) were grown from THF. ^{11}B-NMR (80 MHz, C_6D_6): δ 2.3 (br t). ^{1}H-NMR (400 MHz, C_6D_6): δ 7.73-7.70 (m, 6H, Ph), 7.29-7.23 (m, 9H, Ph), 5.77 (s, 10H, Cp), 2.23-1.75 (m, 13H, β-, γ-, μ-H), 1.47 (br s, 2H, α-H), 0.5 (br s, 1H, μ-H). ^{13}C-NMR (101 MHz, C_6D_6): δ 138.1 (s, Ph), 135.5 (s, Ph), 129.8 (s, Ph), 128.1 (s, Ph), 110.4 (Cp), 34.1 (s, β-C), 27.8 (br s, α-C), 25.2 (br s, γ-C). IR (KBr, cm^{-1}): 3119 (vw), 3063 (w), 3044 (w), 3020 (w), 2994 (w), 2952 (w), 2925 (mw), 2867 (m), 2823 (m), 2164 (vw), 2054 (m), 2022 (m, sh), 1943 (m), 1889 (mw, sh), 1818 (w), 1746 (vw), 1587 (mw), 1484 (m), 1441 (m, sh), 1428 (s), 1407 (ms, sh), 1386 (s), 1343 (s), 1310 (w, sh), 1281 (mw), 1204 (mw), 1187 (w), 1110 (s), 1070 (m), 1023 (ms), 1015 (ms), 1001 (s, sh), 972 (vs), 927 (s, sh), 839 (ms), 814 (s), 799 (s, sh), 745 (s), 736 (m, sh), 710 (s), 612 (mw), 526 (ms, sh), 512 (s), 457 (ms) cm^{-1}. Anal. Calc. for $C_{36}H_{41}BHfOSi$: C, 61.15; H, 5.84. Found: C, 61.75; H, 6.27%.

3.8. Reaction of 1 with K[H₂BC₈H₁₄]. Formation of [Cp₂Ti(μ-Cl)₂TiCp₂] (6)

A 50 ml flask was charged with 0.272 g (0.556 mmol) of **1**, 0.091 g (0.56 mmol) of $K[H_2BC_8H_{14}]$, and 15 ml of Et_2O. The mixture was stirred for 3 h, during which time the solution changed color from orange to purple to dark green and hydrogen evolved. Filtration of the solution and slow removal of the solvent under vacuum at r.t. afforded green crystals. The mother liquor (2 ml) was removed and the crystals were washed with 3 × 5 ml of cold hexane (ca. -40 °C) and dried under dynamic vacuum for 3 h (152 mg, 64% yield). ^{1}H-NMR (250 MHz, C_6D_6): not valid. ^{13}C-NMR (63 MHz, C_6D_6): not valid.

4. Supplementary material

Crystallographic data for the structural analysis (excluding structure factors) have been deposited with the Cambridge Crystallographic Data Centre, CCDC nos. 211361–211364 for compounds **3**–**6**. Copies of this information may be obtained free of charge from The Director, CCDC, 12 Union Road, Cambridge CB2 1EZ, UK (Fax: +44-1223-336033; e-mail: deposit@ccdc.cam.ac.uk or www: http://www.ccdc.cam.ac.uk).

Acknowledgements

References

[1] Supported Group IV organometallics: (a) M. Jezequel, V. Dufaud, M.J. Ruiz-Garcia, F. Carrillo-Hermosilla, U. Neuge-bauer, G.P. Niccolai, F. Lefebvre, F. Bayard, J. Corker, S. Fiddy, J. Evans, J.P. Broyer, J. Malinge, J.-M. Basset, J. Am. Chem. Soc. 123 (2001) 3520;
(b) F. Quignard, C. Lecuyer, C. Bougault, F. Lefebvre, A. Choplin, D. Olivier, J.-M. Basset, Inorg. Chem. 31 (1992) 928;
(c) S.A. King, J. Schwartz, Inorg. Chem. 30 (1991) 3771;
(d) C. Rosier, G.P. Niccolai, J.-M. Basset, J. Am. Chem. Soc. 119 (1997) 12408;
(e) S.A. Holmes, F. Quignard, A. Choplin, R. Teissier, J. Kervennal, J. Catal. 176 (1998) 173;
(f) L. d'Ornelas, S. Reyes, F. Quignard, A. Choplin, J.-M. Basset, Chem. Lett. (1993) 1931.
[2] Supported organolanthanides: (a) W.C. Finch, R.D. Gillespie, D. Hedden, T.J. Marks, J. Am. Chem. Soc. 112 (1990) 6221;
(b) P.J. Toscano, T.J. Marks, J. Am. Chem. Soc. 107 (1985) 653.
[3] A recent review on surface organometallic chemistry: C. Copéret, M. Chabanas, R.P. Saint-Arroman, J.-M. Basset, Angew. Chem. Int. Ed. 42 (2003) 156.
[4] Reviews: (a) F.J. Feher, T.A. Budzichowski, Polyhedron 14 (1995) 3239;
(b) H.C.L. Abbenhius, Chem. Eur. J. 6 (2000) 25;
(c) R. Duchateau, Chem. Rev. 102 (2002) 3525.
[5] (a) R. Duchateau, H.C.L. Abbenhius, R.A. van Santen, S.K.-H. Thiele, M.F.H. van Tol, Organometallics 17 (1998) 5222;
(b) R. Duchateau, U. Cremer, R.J. Harmsen, S.I. Mohamud, H.C.L. Abbenhius, R.A. van Santen, A. Meetsma, S.K.-H. Thiele, M.F.H. van Tol, M. Kranenburg, Organometallics 18 (1999) 5447.
[6] (a) H.C. Brown, S. Krishnamurthy, Tetrahedron 35 (1979) 567;
(b) S.G. Shore, J. Liu, G.T. Jordan, IV, F.-C. Liu, E.A. Meyers, P.L. Gaus, Cyclic organohydroborate anions as hydride transfer agents in reactions with organic and organometallic compounds, in: W. Siebert (Ed.), Advances in Boron Chemistry, The Royal Society of Chemistry, London, 1997, pp. 84–91.
[7] See, for example: (a) P. Zanella, F. Ossola, M. Porchia, G. Rossetto, A.C. Villa, C. Guastini J. Organomet. Chem. 323 (1987) 295;
(b) R.E.v.H. Spence, W.E. Piers, Y. Sun, M. Parvez, L.R. MacGillivray, M.J. Zaworotko, Organometallics 17 (1998) 2459;
(c) D.R. Lantero, D.L. Ward, M.R. Smith III, J. Am. Chem. Soc.
119 (1997) 9699;
(d) A. Antiñolo, F. Carrillo-Hermosilla, J. Fernández-Baeza, S. García-Yuste, A. Otero, A.M. Rodríguez, J. Sánchez-Prada, E. Villaseñor, R. Gelabert, M. Moreno, J.M. Lluch, A. Lledós, Organometallics 19 (2000) 3654;
(e) P.A. Chase, W.E. Piers, M. Parvez, Organometallics 19 (2000) 2040.
[8] (a) G.T. Jordan, IV, S.G. Shore, Inorg. Chem. 35 (1996) 1087;
(b) G.T. Jordan, IV, F.-C. Liu, S.G. Shore, Inorg. Chem. 36 (1997) 5597;
(c) J. Liu, E.A. Meyers, S.G. Shore, Inorg. Chem. 37 (1998) 496;
(d) F.-C. Liu, J. Liu, E.A. Meyers, S.G. Shore, Inorg. Chem. 37 (1998) 3293;
(e) F.-C. Liu, J. Liu, E.A. Meyers, S.G. Shore, Inorg. Chem. 38 (1999) 2169;
(f) F.-C. Liu, B. Du, J. Liu, E.A. Meyers, S.G. Shore, Inorg. Chem. 38 (1999) 3228;
(g) F.-C. Liu, C.E. Plecnik, S. Liu, J. Liu, E.A. Meyers, S.G. Shore, J. Organomet. Chem. 627 (2001) 109;
(h) X. Chen, S. Liu, C.E. Plenik, F.-C. Liu, G. Fraenkel, S.G. Shore, Organometallics 22 (2003) 275.
[9] (a) S.G. Shore, F.-C. Liu, Cationic metallocenes derived from cyclic organohydroborate metallocene complexes, in: M.G. Davidson, A.K. Hughes, T.B. Marder, K. Wade (Eds.), Contemporary Boron Chemistry, The Royal Society of Chemistry, London, 2000, pp. 28–35;
(b) A. Chow, F.-C. Liu, G. Fraenkel, S.G. Shore, Magn. Reson. Chem. 36 (1998) 145.
[10] E.Y.-X. Chen, T.J. Marks, Chem. Rev. 100 (2000) 1391.
[11] (a) S. Liu, F.-C. Liu, G. Renkes, S.G. Shore, Organometallics 20 (2001) 5717;
(b) C.E. Plecnik, F.-C. Liu, S. Liu, J. Liu, E.A. Meyers, S.G. Shore, Organometallics 20 (2001) 3599;
(c) F.-C. Liu, J. Liu, E.A. Meyers, S.G. Shore, J. Am. Chem. Soc. 122 (2000) 6106.
[12] Recent reviews of cationic metallocenes and olefin polymerization: (a) A thematic issue on the subject, Chem. Rev. 100 (14) (2000);
(b) H.C.L. Abbenhius, Angew. Chem. Int. Ed. 38 (1999) 1058;
(c) A.L. McKnibht, R.M. Waymouth, Chem. Rev. 98 (1998) 2587;
(d) W. Kaminsky, J. Chem. Soc. Dalton Trans. (1998) 1413;
(e) M. Bochmann, J. Chem. Soc. Dalton Trans. (1996) 255.
[13] D.W. von Gudenburg, H.-C. Kang, W. Massa, K. Dehnicke, C. Maichle-Mössmer, J. Strähle, Z. Anorg. Allg. Chem. 620 (1994) 1719.
[14] (a) A. Haoudi-Mazzah, P. Dhamelincourt, J. Gnado, A. Mazzah, J. Raman Spectrosc. 26 (1995) 1027;
(b) A. Haoudi-Mazzah, A. Mazzah, J. Gnado, P. Dhamelincourt, J. Raman Spectrosc. 27 (1996) 451.
[15] R. Köster, G. Seidel, Inorg. Synth. 22 (1983) 198.
[16] F.-C. Liu, Ph.D. Dissertation, The Ohio State University, 1998.
[17] (a) C.D. Good, D.M. Ritter, J. Am. Chem. Soc. 84 (1962) 1162;
(b) H. Nöth, B. Wrackmeyer, Nuclear Magnetic Resonance Spectroscopy of Boron Compounds (Table 9.3), Springer-Verlag, Berlin, 1978, pp. 115–124 (Table 9.3).
[18] R. Jungst, D. Sekutowski, J. Davis, M. Luly, G. Stucky, Inorg. Chem. 16 (1977) 1645.
[19] (a) J.A. Connor, Top. Curr. Chem. 71 (1977) 71;
(b) M.F. Lappert, D.S. Patil, J.B. Pedley, J. Chem. Soc. Chem. Comm. (1975) 830;
(c) Mean bond dissociation enthalpies are for homoleptic ML_n compounds; $OR = OPr^i$.
[20] (a) H. Nöth, R. Hartwimmer, Chem. Ber. 93 (1960) 2238;
(b) C.R. Lucas, Inorg. Synth. 17 (1977) 91.
[21] R. Köster, M. Yalpani, J. Org. Chem. 51 (1986) 3054.

[22] E.A. Babaian, D.C. Hrncir, S.G. Bott, J.L. Atwood, Inorg. Chem. 25 (1986) 4818.

[23] Z. Otwinowsky, W. Minor, Processing of X-ray diffraction data collected in oscillation mode, in: C.W. Carter, Jr., R.M. Sweet (Eds.), Macromolecular Crystallography Part A Methods in Enzymology, vol. 276, Academic Press, New York, 1997, pp. 307–326.

[24] (a) R.H. Blessing, Acta Crystallogr. Sect. A 51 (1995) 33;
(b) R.H. Blessing, J. Appl. Crystallogr. 30 (1997) 421.

[25] S. Mackay, C.J. Gilmore, C. Edwards, M. Tremayne, N. Stuart, K. Shankland, MaXus: A Computer Program for the Solution and Refinement of Crystal Structures from Diffraction Data, University of Glasgow, Scotland, Nonius BV, Delft, The Netherlands, MacScience, Yokohama, Japan, 1998.

[26] G.M. Sheldrick, SHELXTL-97: A Structure Solution and Refinement Program, University of Göttingen, Germany, 1998.

[27] S. Parsons, B. Gould, R. Cooper, L. Farrugia, ROTAX, Version 26, University of Edinburgh, Scotland, 2001.

[28] G.H. Stout, L.H. Jensen, X-ray Structure Determination, second ed., Wiley, New York, 1989, pp. 406–408. The standard deviation (Φ_l) for the average bond lengths is calculated according to the following equations from Ref. [27]: $\Phi_l = 3_m \ [(l_m \pm l)^2/m(m-1)]^{1/2}$ where $+l$ is the mean length, l_m is the length of the mth bond, and m is the number of bonds. The standard deviation is written in brackets.